Quantitative analysis of the kinetics of denaturation and renaturation of barstar in the folding transition zone

M.C.R. SHASTRY, VISHWAS R. AGASHE, AND JAYANT B. UDGAONKAR

National Centre For Biological Sciences, TIFR Centre, Indian Institute of Science Campus, Bangalore 560012, India

Abstract

The fluorescence-monitored kinetics of folding and unfolding of barstar by guanidine hydrochloride (GdnHCl) in the folding transition zone, at pH 7, 25 °C, have been quantitatively analyzed using a 3-state mechanism: $U_S \rightleftharpoons U_F \rightleftharpoons N$. U_S and U_F are slow-refolding and fast-refolding unfolded forms of barstar, and N is the native protein. U_S and U_F probably differ in possessing *trans* and *cis* conformations, respectively, of the Tyr 47–Pro 48 bond. The 3-state model could be used because the kinetics of folding and unfolding of barstar show 2 phases, a fast phase and a slow phase, and because the relative amplitudes of the 2 phases depend only on the final refolding conditions and not on the initial conditions. Analysis of the observed kinetics according to the 3-state model yields the values of the 4 microscopic rate constants that describe the transitions between the 3 states at different concentrations of GdnHCl. The value of the equilibrium unfolded ratio $U_S:U_F$ (K_{21}) and the values of the rate constants of the $U_S \rightarrow U_F$ and $U_F \rightarrow U_S$ reactions, k_{12} and k_{21}, respectively, are shown to be independent of the concentration of GdnHCl. K_{21} has a value of 2.1 ± 0.1, and k_{12} and k_{21} have values of 5.3×10^{-3} s^{-1} and 11.2×10^{-3} s^{-1}, respectively. Double-jump experiments that monitor reactions that are silent to fluorescence monitoring were used to confirm the values of K_{21}, k_{12}, and k_{21} obtained from the 3-state analysis and thereby the validity of the 3-state model. The 3-state model does not account for the kinetics of folding in the pretransition region, where folding occurs by 2 parallel pathways, $U_F \rightarrow N$, and $U_S \rightarrow I_N \rightarrow N$, and I_N is a native-like intermediate. The rate constants of the $U_F \rightarrow N$ and $U_S \rightarrow I_N$ reactions are both similar, with values of 37 s^{-1} in water. The $I_N \rightarrow N$ reaction, which involves the same *trans-cis* isomerization process as the $U_S \rightarrow U_F$ reaction, occurs with a rate constant of 16×10^{-3} s^{-1} and is independent of GdnHCl concentration. Thus, *trans-cis* isomerization occurs 3 times faster in the folding intermediate than in the unfolded state.

Keywords: barstar; denaturation; folding pathway; proline isomerization

The method of choice for studying the folding pathway of a protein is to dissect the complex folding reaction into simpler steps that involve folding intermediates. In general, equilibrium folding intermediates are not found to exist in conditions where the protein is functionally active. The most common equilibrium folding intermediate, the molten globule intermediate, is usually formed only at extremes of pH, ionic strength, or temperature (reviewed by Kuwajima, 1992). Kinetic intermediates have, however, been identified on the folding pathway of many proteins (reviewed by Kim & Baldwin, 1990; Matthews, 1993) in native-like conditions and, in the case of small proteins, methods now exist to obtain structural information on these intermediates (Roder et al., 1988; Udgaonkar & Baldwin, 1988; Matouschek & Fersht, 1991; Evans & Radford, 1994).

The small protein barstar is being used as a model protein for folding studies in our laboratory. Barstar is an 89-residue protein found in *Bacillus amyloliquefaciens*, where it functions as an inhibitor to barnase, a ribonuclease secreted by the same organism (Hartley, 1988). It has been shown to bind to barnase with a 1:1 stoichiometry, with a dissociation constant in the picomolar region (Hartley, 1993; Schreiber & Fersht, 1993a). Although crystals of barstar have been obtained (Guillet et al., 1993b), an X-ray crystal structure is still awaited. The structure of the complex of barnase with a mutant form of barstar, BSCCAA, in which the 2 cysteine residues were replaced by alanines, has, however, been solved and shows barstar to possess 4 α-helices and 3 β-strands (Guillet et al., 1993a). Two-

dimensional NMR assignment studies (Lubienski et al., 1993; S. Ramachandran, S. Mayo, & J.B. Udgaonkar, unpubl. results) also indicate the presence of 4 α-helices in solution. At low pH, barstar adopts a molten globule-like form (Khurana & Udgaonkar, 1994), which has been characterized in some detail.

The folding pathway of BSCCAA, a mutant barstar protein, in which the 2 cysteine residues of barstar are replaced by alanines, has been studied in detail by Schreiber and Fersht (1993b) at pH 8, using urea as the denaturant. In that elegant study, the focus was on the mechanism of folding in the pretransition zone, and 2 parallel folding pathways were identified:

$$U_F \rightarrow N \qquad \text{(Mechanism 1)}$$

$$U_S \rightarrow I_N \rightarrow N. \qquad \text{(Mechanism 2)}$$

U_F and U_S, referred to as U_C and U_T, respectively, by Schreiber and Fersht (1993b), are the 2 unfolded forms of barstar, with U_F (the fast-refolding form) folding at least 500-fold faster than U_S (the slow-refolding form). The 2 unfolded forms probably differ in the Tyr 47–Pro 48 bond being in the native *cis* conformer in U_F and in the non-native *trans* conformer in U_S (Schreiber & Fersht, 1993b). I_N (I_{2T}) is a native-like intermediate that was shown to be able to inhibit barnase. Very early intermediates (I_1) were also implicated on both the folding pathways, but there are no direct data on their role on the folding pathways (Schreiber & Fersht, 1993b).

In this paper, the focus is on the quantitative analysis of the unfolding and refolding of barstar in both the folding transition zone and the posttransition zone of denaturant concentration. A 3-state model for unfolding and refolding, $N \rightleftharpoons U_F \rightleftharpoons U_S$ was used to analyze the data. The thermal denaturation of ribonuclease A (Hagerman & Baldwin, 1976) and the GdnHCl-induced denaturation of an immunoglobulin light chain (Goto & Hamaguchi, 1982) have previously been quantitatively analyzed on the basis of such a model. In this report, the observed kinetics of folding and unfolding of barstar have been analyzed according to the 3-state model to obtain the 4 microscopic rate constants that characterize the model. The values of the microscopic rate constants so obtained have been confirmed by double-jump experiments and, hence, the validity of the 3-state analysis established.

Results

Figure 1 compares the denaturation curve obtained from kinetic experiments ($F_1 + F_2$) to that obtained from equilibrium experiments. The kinetic and equilibrium data are coincident: the entire fluorescence change seen in an equilibrium experiment is also detected in the kinetic experiment. The data can be fit to a 2-state transition (Equation 1) and the value for C_M, the midpoint of the unfolding transition, obtained (1.9 M) is identical to that reported previously using both CD and fluorescence as the probes for monitoring folding (Khurana & Udgaonkar, 1994).

The folding of barstar, when measured using final GdnHCl concentrations in the pretransition and transition zones, is biphasic. Similarly, the unfolding of barstar is biphasic when measured using GdnHCl concentrations in the transition zone, but can be described by a single first-order process in the posttransition zone. In both of the cases, the fast phase is at least 500-fold faster than the slow phase at all concentrations of GdnHCl
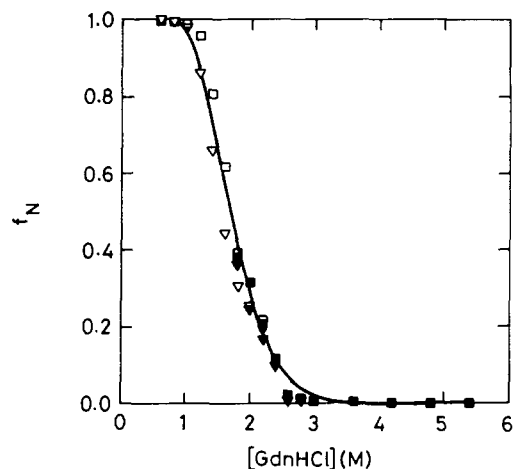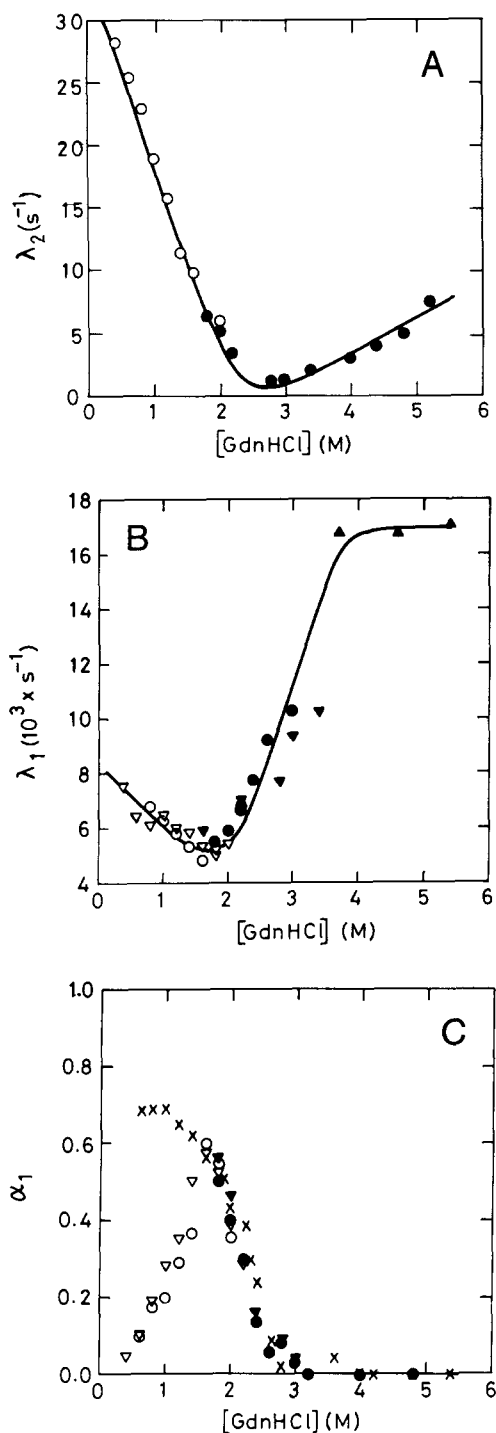

Fig. 1. GdnHCl-induced unfolding of barstar at pH 7, 25 °C. Unfolding was followed by monitoring intrinsic tryptophan fluorescence at 320 nm on excitation at 287 nm. The apparent fraction of native protein, f_N, calculated according to Equation 1, is plotted against GdnHCl concentration. Open symbols are from refolding experiments and closed symbols are from unfolding experiments. Data points obtained from an equilibrium denaturation curve are given by $\square$ and $\blacksquare$. The protein was incubated at various GdnHCl concentrations for 2 h before measurement of fluorescence. Data points obtained from kinetic experiments as the sum of the amplitudes ($F_1 + F_2$) of the 2 phases observed in folding and unfolding experiments are given by $\triangledown$ and $\blacktriangledown$. The data were fit to a 2-state model for unfolding according to Equation 1. The solid line through the data represents such a fit with $m_G = 2.6$ kcal mol^{-1} M^{-1} and $\Delta G(H_2O) = 4.9$ kcal mol^{-1}.

used. The GdnHCl concentration dependencies of the rate constants of the 2 phases, and of the relative amplitude of the slow phase, are shown in Figure 2.

In Figure 2A is shown the dependence of the apparent rate constant of the fast phase of folding and unfolding, λ_2, on the concentration of the denaturant. λ_2 shows a minimum around a GdnHCl concentration of 2.5 M. Extrapolation of the λ_2 values in the pretransition region to zero GdnHCl concentration, using Equation 5, yields a value for the folding rate constant for the fast phase when refolded in 0 M GdnHCl, $\lambda_2(H_2O)$ (folding), of 37 s^{-1}. This value is similar to that reported for BSCCAA (31 s^{-1}) (Schreiber & Fersht, 1993b). In the posttransition region too, λ_2 is found to increase with increasing GdnHCl concentration according to Equation 5, and the value of the unfolding rate constant extrapolated to 0 M GdnHCl $\lambda_2(H_2O)$ (unfolding) is 0.096 s^{-1}.

In Figure 2B is shown the dependence of λ_1, the apparent rate constant of the slow phase of folding and unfolding, on GdnHCl concentration. λ_1 increases marginally with decreasing GdnHCl concentration in the pretransition zone and exhibits a broad minimum around 1.7 M GdnHCl, above which it increases again.

Figure 2C shows the relative amplitude of the slow phase, α_1, as a function of GdnHCl concentration. At very low GdnHCl concentrations, over 95% of the folding reaction occurs in the fast phase. α_1 increases sharply with increasing GdnHCl concentration (see Discussion for an explanation) and shows a maximum at a GdnHCl concentration of 1.9 M, which is also the midpoint of the unfolding transition (Fig. 1). In the posttransition region (>3 M GdnHCl), more than 98% of the unfold-

ing reaction occurs in the fast phase, and hence the data were fit to a single-exponential decay.

Identical values are obtained for both λ_1 and λ_2 regardless of whether they are obtained from a folding or an unfolding experiment (Fig. 2A,B), indicating that the apparent rate constants depend only on the final conditions and not on the initial conditions, which is expected for a fully reversible folding/unfolding process. Similarly, α_1 is the same whether obtained from a folding or from an unfolding experiment: its value is independent of the initial conditions and depends only on the final conditions of folding or unfolding. The values for λ_1 and α_1 in the transition region obtained using manual mixing experiments agree with those obtained using stopped-flow mixing experiments (see Fig. 2).

Formation of two unfolded species

To determine whether the slow phase of folding was due to the presence of an intermediate on the folding pathway or was due to the presence of 2 unfolded forms of barstar, double-jump experiments were carried out, as shown in Figure 3. Barstar was subjected to an unfolding pulse of varying duration in 5.4 M GdnHCl before being refolded in 1.35 M GdnHCl. Figure 2A indicates that barstar is completely unfolded within 1 s of incubation in 5.4 M GdnHCl (λ_2 [unfolding] = 7 s^{-1}), and that under the refolding conditions of 1.35 M GdnHCl almost all the molecules refold completely. The large value of α_1 under these conditions simplifies monitoring of the slow phase of folding. Figure 3 shows that the amplitude of the slow phase in folding increases exponentially with the time of prior unfolding, from zero at zero time, with an apparent rate constant of $17 \pm 2 \times 10^{-3}$ s^{-1}. This experiment was repeated with 3.7 M GdnHCl and 4.6 M GdnHCl being used to unfold the protein. The values of the apparent rate constants obtained are similar to those
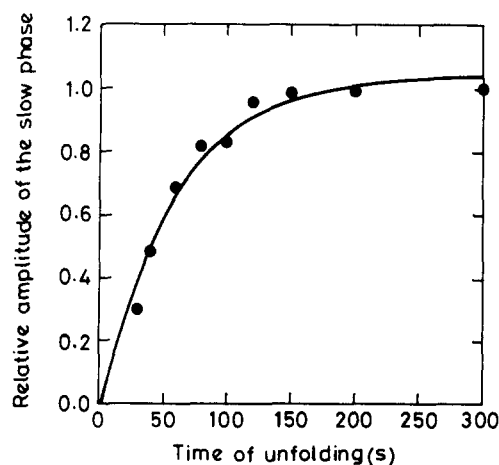
Fig. 2. Kinetics of folding and unfolding of barstar at pH 7, 25 °C. Open symbols refer to data obtained from folding experiments. Closed symbols refer to data obtained from unfolding experiments. Data obtained from stopped-flow mixing experiments are given by O and ●. Data obtained from manual mixing experiments are given by ▽ and ▼. Data obtained from double-jump experiments as illustrated in Figure 3 are given by ▲. Values for α_1 calculated using Equation 11 with f_N determined from equilibrium measurements (Fig. 1) are given by X. **A:** Rate constant of the fast phase in folding and unfolding, λ_2. **B:** Rate constant of the slow phase in folding and unfolding, λ_1. **C:** Relative amplitude of the slow phase, α_1. The solid lines in A and B have been drawn by inspection only. All measurements had a standard deviation of $\pm 10\%$.

Fig. 3. Double-jump experiment monitoring the U_F to U_S transition at pH 7, 25 °C. After different times of unfolding in 5.4 M GdnHCl, indicated in the figure, the unfolded protein solution was diluted to a final GdnHCl concentration of 1.35 M GdnHCl and the refolding kinetics measured by monitoring fluorescence at 320 nm. The amplitude of fluorescence change in the slow phase of refolding relative to that observed on complete unfolding of the protein in 5.4 M GdnHCl is plotted against the duration of the unfolding pulse prior to refolding. The solid line through the data indicates a fit to a single exponential and yields an apparent rate constant of 17×10^{-3} s^{-1}.

obtained with 5.4 M GdnHCl and are shown in Figure 2B. These results indicate that 2 unfolded forms of barstar exist. One form, U_F, refolds fast, and another form, U_S, refolds slowly. On unfolding, U_F is first formed and it slowly converts to U_S with an apparent rate constant of 17×10^{-3} s^{-1}, which is independent of the concentration of GdnHCl used to unfold the protein.

Determination of the equilibrium ratio of U_S to U_F in unfolded barstar

Figure 4A shows the results of a double-jump experiment in which barstar that had been first unfolded to equilibrium in 6 M GdnHCl was allowed to refold in 1.2 M GdnHCl for 20 s before being re-unfolded in 3.7 M GdnHCl. The second unfolding is observed to be biphasic. This indicates that there are 2 fully folded or partly folded structures present. A partly folded structure (intermediate) is expected to unfold faster than the fully folded protein. The slower phase has the same rate of unfolding (4 s^{-1}) as the rate of unfolding of N in 3.7 M GdnHCl determined in the direct unfolding experiment (Fig. 2A). The faster phase has a rate constant of 28 s^{-1}. The amplitudes of the 2 unfolding phases observed account for the entire re-unfolding reaction.

To confirm that the slower of the 2 phases shown in Figure 4A does indeed correspond to the unfolding of N, the concentration of GdnHCl used to finally unfold the protein after 1 s of folding was varied from 3 M to 4.2 M. The dependence of the 2 unfolding rate constants observed on GdnHCl concentration is shown in Figure 4B. Also shown in Figure 4B are the rate constants (λ_2) observed in direct unfolding experiments, which are from Figure 2A. Figure 4B clearly indicates that the slower of the 2 observed rate constants does indeed correspond to the rate constant of unfolding of N. Thus, the amplitude of the slower phase corresponds to the amount of N that is present at the time of re-unfolding.

The faster of the 2 observed rate constants is approximately 10-fold faster at all GdnHCl concentrations. This faster unfolding phase reflects the unfolding of the native-like intermediate, I_N, that has formed, and the amplitude of the faster phase therefore reflects the amount of I_N that is present at the time of re-unfolding. Native-like intermediates have been similarly detected in the case of ribonuclease A (Schmid, 1983), ribonuclease T1 (Kiefhaber & Schmid, 1992), and also BSCCAA (Schreiber & Fersht, 1993b).

The time of refolding before re-unfolding with 3.7 M GdnHCl was varied from 1 to 300 s, and the amounts of N and I_N at each time are determined from the amplitudes of the respective phases of re-unfolding. Figure 5 shows the change in concentrations of N and I_N with time. The amount of N is seen to increase from 31% at 1 s to 100% in a single first-order process with a rate constant of 16×10^{-3} s^{-1}, and the amount of I_N decreases from 69% at 1 s to 0% at approximately the same rate. At all times from 1 to 300 s, N and I_N are the only 2 species present. Figure 5 indicates that 31% of the molecules form N in a fast-folding reaction. In the case of BSCCAA also (Schreiber & Fersht, 1993b), the same technique shows that 30% of the molecules have formed N in a fast-folding reaction.

Discussion

Many proteins denature to 2 or more unfolded forms that refold at different rates (Garel & Baldwin, 1973; Schmid, 1986a;
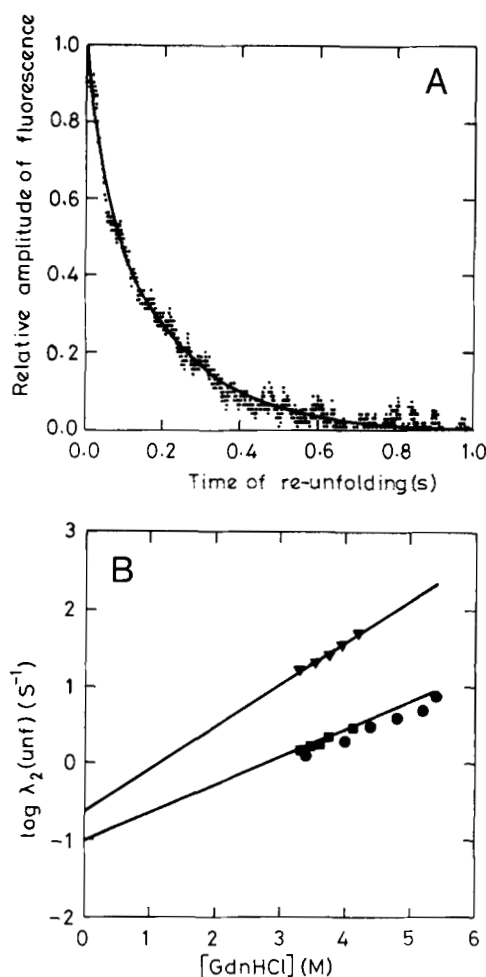
Fig. 4. A: Double-jump experiment showing the presence of N and I_N. Barstar was first unfolded to equilibrium in 6 M GdnHCl and then folding was commenced by dilution of the GdnHCl to 1.2 M. After 20 s of refolding, the folding protein solution was subject to an unfolding assay in which the GdnHCl concentration was raised to 3.7 M and the kinetics of re-unfolding were monitored. The change in fluorescence on re-unfolding relative to the total change observed if the protein were allowed to refold completely before application of the unfolding assay is plotted versus time of re-unfolding. The solid line through the data is a least-squares fit of the data to a double-exponential process, and the fitted line is described by the equation: $A(t) = 0.6 * \exp(-28t) + 0.4 * \exp(-4t)$. **B:** GdnHCl concentration dependence of the rate constants of unfolding of I_N and N. After first unfolding to equilibrium in 6 M GdnHCl, the protein was refolded for 1 s in 0.6 M GdnHCl before being re-unfolded using the concentrations of GdnHCl indicated. A biphasic unfolding curve was observed in each case. The faster of the 2 phases accounted for 69% of the total unfolding amplitude and the slower of the 2 phases accounted for 31% of the total unfolding amplitude. The rate constants of the faster (▼) and the slower (■) phases of re-unfolding observed are plotted as a function of GdnHCl concentration. Also plotted are the rate constants of unfolding of N from Figure 2A (●). The straight lines through the data are fits of each set of rate constants to Equation 5. For the fast phase of unfolding, $\lambda_2(H_2O) = 0.24$ s^{-1} and $m_{\lambda 2} = 0.62$ M^{-1}; for the slow phase, $\lambda_2(H_2O) = 0.096$ s^{-1} and $m_{\lambda 2} = 0.36$ M^{-1}.

Kiefhaber et al., 1992). The presence of slow-folding and fast-refolding forms has been explained on the basis of *cis–trans* isomerization of X–Pro bonds (Brandts et al., 1975). If all such bonds are in the same conformation in the unfolded state as in
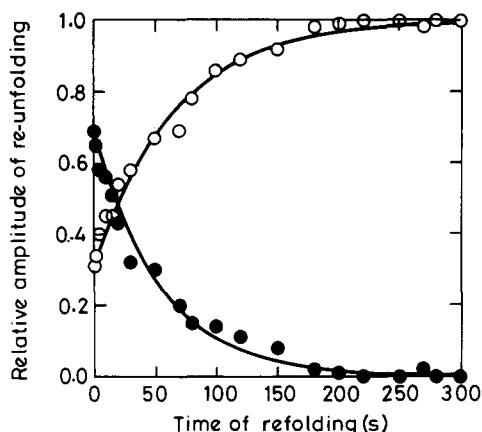
Fig. 5. Double-jump experiment monitoring the folding of U_S. Barstar was unfolded to equilibrium in 6 M GdnHCl. Folding was initiated by dilution of the unfolded protein solution to a final GdnHCl concentration of 1.2 M. After different times of refolding from 1 to 300 s, the protein was re-unfolded with 3.7 M GdnHCl. The amplitudes of the 2 phases of unfolding that were observed in each unfolding reaction, relative to the total unfolding amplitude observed when the refolding reaction was allowed to go to completion, are plotted against the duration of the refolding pulse. The solid line through the data for the slower of the 2 phases (O), corresponding to the unfolding of N (see text), is a fit of the data to a single exponential process and is described by $N(t) = 1 - 0.69*\exp(-0.016t)$, where $N(t)$ is the amplitude of unfolding of N at time t and is equal to the fraction of N at t seconds. The solid line through the data for the faster of the 2 phases ($\bullet$), corresponding to the unfolding of I_N (see text), is also a fit of the data to a single exponential process and is described by $I_N(t) = 0.69*\exp(-0.017t)$.

the fully folded state, then the unfolded form can refold rapidly. In contrast, if the unfolded form has X-Pro bonds in a non-native conformer, then folding is slowed down by *cis-trans* isomerization. Replacement of *cis* prolines in ribonuclease A (Schultz et al., 1992), ribonuclease T1 (Kiefhaber et al., 1990), staphylococcal nuclease (Nakano et al., 1993), and thioredoxin (Kelley & Richards, 1987) leads to the elimination of the slow-refolding reactions in these proteins. This effect is, however, not seen in the case of human lysozyme (Herning et al., 1991), indicating that factors other than *cis-trans* isomerization of X-Pro bonds could also be responsible for slow-folding reactions in some proteins. In the case of BSCCAA, the rate of the slow-refolding reaction increases more than 10-fold in the presence of the enzyme prolyl isomerase, which catalyzes *cis-trans* isomerization of X-Pro bonds in small peptides. Although the enzyme had to be used in equimolar amounts, this result strongly indicates that the 2 unfolded forms differ in possessing different conformers of at least 1 X-Pro bond. Barstar has 2 proline residues, of which Pro 48 has been shown to be *cis* in the fully folded protein (Lubienski et al., 1993). Because X-Pro bonds usually are *trans* in the unfolded state (Grathwohl & Wüthrich, 1976), it was suggested that the Tyr 47-Pro 48 bond is *cis* in U_F and *trans* in U_S (Schreiber & Fersht, 1993b).

The kinetics of both the folding and unfolding of barstar by GdnHCl at pH 7, 25 °C, are biphasic. One phase is at least 500-fold faster than the other over the entire range of GdnHCl (Fig. 2). The kinetics are broadly similar to the kinetics reported earlier for BSCCAA at pH 8, 25 °C, with urea as the denaturant (Schreiber & Fersht, 1993b). In that study of BSCCAA folding

kinetics, however, a quantitative analysis of the data according to a 3-state model of folding in the folding transition zone and posttransition zone was not attempted, even though the data passed 2 basic requirements of a 3-state model: both a slow phase and a fast phase were observed in folding and unfolding, and the relative amplitudes of a folding experiment and an unfolding experiment to the same final conditions were the same. The data in Figure 2 show that these 2 basic requirements are fulfilled in the case of barstar also, allowing a quantitative 3-state analysis to be carried out.

Formation of 2 unfolded species

Double-jump experiments such as that shown in Figure 3 were used to confirm the presence of 2 unfolded forms of barstar. Such double-jump experiments unequivocally demonstrate that, upon unfolding, barstar first forms the fast-refolding form, U_F, which then slowly converts to the slow-refolding form, U_S, resulting in an equilibrium unfolded mixture of U_F and U_S. These double-jump experiments also allow the monitoring of the slow phase of unfolding outside the folding transition zone and, consequently, the determination of the kinetics of the U_F to U_S transition. These experiments were not reported in the study on BSCCAA (Schreiber & Fersht, 1993b).

The 3-state model (Mechanism 3) was therefore used for a quantitative analysis of the kinetics of folding and unfolding of barstar by GdnHCl in the folding transition zone at pH 7, 25 °C. The equations relating the microscopic rate constants to the observed rates and amplitudes have been reproduced in the Materials and methods section. The individual microscopic rate constants were first determined at different GdnHCl concentrations, using the observed values of λ_1, λ_2, α_1, and f_N at each GdnHCl concentration, and Equations 6, 7, 8, and 13. It should be noted that no limiting conditions have been applied to any of these 4 equations. The values of the 4 microscopic rate constants are plotted against GdnHCl concentration in Figure 6.
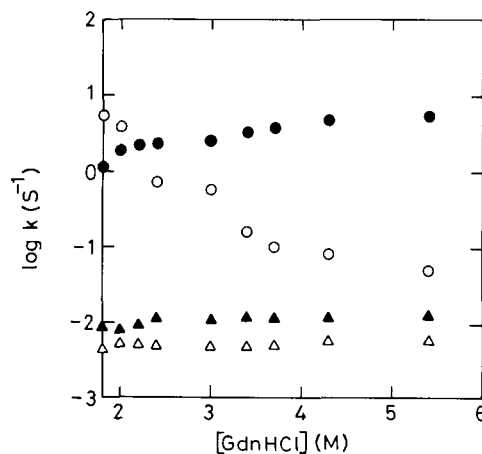
Fig. 6. Dependence of the microscopic rate constants characterizing the 3-state model on GdnHCl concentration. The 4 microscopic rate constants k_{12} ($\triangle$), k_{21} ($\blacktriangle$), k_{23} (O), and k_{32} ($\bullet$) are plotted versus GdnHCl concentration. The microscopic rate constants were determined at each GdnHCl concentration using Equations 6, 7, 8, and 13 and the data in Figures 1 and 2.

It is seen that k_{23} and k_{32} have a strong dependence on GdnHCl concentration. This is expected because these are the rate constants that characterize the actual folding and unfolding of the protein. The determination of k_{23} and k_{32} at each GdnHCl concentration yielded the true equilibrium constant K_{32} for the folding reaction ($U_F \rightleftharpoons N$). λ_2 is at a minimum at approximately the GdnHCl concentration (2.5 M) where $k_{23} = k_{32}$. The 2-state analysis of the equilibrium denaturation curve in Figure 1 yields only the apparent equilibrium constant, K_{app}, which is defined in Equation 12, and is therefore larger than the true equilibrium constant for the folding process, K_{32}.

The rate constants k_{12} and k_{21} are seen not to depend on GdnHCl concentration, as expected for rate constants characterizing *cis-trans* isomerization of a Pro residue in an unfolded protein. This result confirms earlier results with ribonuclease A (Schmid & Baldwin, 1979), which had shown $k_{12} + k_{21}$ to be independent of GdnHCl concentration in the posttransition zone. The validity of the 3-state model was established by direct determination of K_{21} and $k_{12} + k_{21}$ from double-jump experiments.

Determination of K_{21}

K_{21} is usually obtained from the determination of α_1 at low denaturant concentrations in the pretransition zone, where α_1 is expected to be constant and equal to $1/(1 + K_{21})$ (Utiyama & Baldwin, 1986). In the cases of both barstar and BSCCAA (Schreiber & Fersht, 1993b), however, U_F folds to N (Mechanism 1), and U_S to the native-like intermediate, I_N (Mechanism 2), with similar fast rate constants, and the entire fluorescence change accompanying the $U_S \rightarrow N$ reaction occurs in the $U_S \rightarrow I_N$ reaction. As a result, the amplitude corresponding to each phase cannot be distinguished and, consequently, α_1 cannot be determined. Moreover, in the case of barstar, α_1 is not constant, but decreases to nearly zero at low concentrations of denaturant in the pretransition zone (see below). A similar result has been seen with BSCCAA (Schreiber & Fersht, 1993b). Thus, the relative amounts of U_F and U_S in equilibrium-unfolded barstar or BSCCAA cannot be determined from α_1, as it can be in the case of ribonuclease A (Garel & Baldwin, 1973; Garel et al., 1976).

A double-jump experiment was therefore devised to determine K_{21} (Schmid, 1986a). Because λ_2 is at least 500-fold faster than λ_1 over the entire range of GdnHCl used, the limiting conditions leading to Equations 9–11 are applicable. In the pretransition zone, $k_{23} \gg k_{32}$, and λ_2 from Equation 10 is therefore equal to k_{23}. The data in Figure 2A therefore indicate that U_F should be completely folded to N within 1 s of refolding at all concentrations of GdnHCl in the pretransition zone. The double-jump experiment shown in Figure 5 determined the amount of N after 1 s of folding in 1.2 M GdnHCl, and at subsequent times of folding, and indicates that 31% of the molecules fold to N within 1 s (Mechanism 1), whereas the remaining 69% of the molecules have rapidly folded to I_N, which then slowly folds to N in a first-order process with a rate constant of 16×10^{-3} s^{-1} (Mechanism 2). The population of unfolded molecules that fold to N within 1 s corresponds to the population of the fast-folding unfolded species, U_F. The remaining population of unfolded molecules that refold slowly is that of the slow-folding unfolded species, U_S. Figure 5 therefore indicates that equilibrium-unfolded barstar consists of 31% U_F and 69% U_S.

When the experiment of Figure 5 was repeated with the folding reaction being carried out in 0.6 M GdnHCl instead of 1.2, with the re-unfolding assay again being done at 3.7 M GdnHCl, the amount of N again increased from 31% at 5 s to 100%, with a rate constant of 16×10^{-3} s^{-1} (data not shown). These results confirm that the equilibrium ratio, U_S:U_F, which is equal to K_{21}, is 69:31, i.e., 2.2:1. They also indicate that the rate-limiting step in the folding of U_S is independent of GdnHCl concentration.

Another type of double-jump experiment, of the type illustrated in Figure 3, yields the apparent rate constant of formation of U_S from U_F, measured to be 17×10^{-3} s^{-1}, which, according to Mechanism 3, is equal to $k_{12} + k_{21}$. This value is shown to be independent of GdnHCl concentration in Figure 2B. According to Equation 9, the value of λ_1 at high concentrations of GdnHCl in the posttransition zone is also equal to $k_{12} + k_{21}$, and the data in Figure 2B suggest that λ_1 approaches the value of $k_{12} + k_{21}$ determined from double-jump experiments as the GdnHCl concentration is increased.

At low concentrations of GdnHCl, where complete refolding occurs, Equation 9 simplifies to $\lambda_1 = k_{12}$. Figure 2B shows that λ_1 increases from a value of 5.2×10^{-3} s^{-1} to 17×10^{-3} s^{-1} across the folding transition zone. Thus, the value of λ_1 increases 3.2-fold across the transition zone. This is the expected increase for a value of 2.2 for K_{21} ($= k_{21}/k_{12}$), if Mechanism 3 is valid for the folding transition zone. The data in Figure 2B therefore confirm the distribution of U_F and U_S in equilibrium-unfolded barstar.

The direct determination of the value of K_{21} (2.2) from the 2 different types of double-jump experiments shown in Figures 3 and 5 and the direct determination of the value of $k_{12} + k_{21}$ (17×10^{-3} s^{-1}) from the double-jump experiment shown in Figure 3 allowed the determination of the individual rate constants k_{12} and k_{21}. k_{12} and k_{21} were calculated to be 5.3×10^{-3} s^{-1} and 11.7×10^{-3} s^{-1}, respectively.

Test of the 3-state model

The validity of the 3-state analysis was tested by comparing the values of K_{21}, k_{12}, and k_{21} obtained from such an analysis with the values determined from the double-jump experiments. Figure 6 shows that the values obtained from a 3-state analysis for k_{12} and k_{21} are independent of GdnHCl concentration and are $5.3 \pm 0.5 \times 10^{-3}$ s^{-1} and $11.2 \pm 1.1 \times 10^{-3}$ s^{-1}, respectively. These values agree very well with the values obtained from the double-jump experiments (see above), and therefore the latter experiments provide a successful test of the 3-state model. It should be noted that a dependence of K_{21} on GdnHCl would have resulted in a noncoincidence of the values obtained for α_1 from unfolding and folding experiments (Hagerman, 1977).

Folding in the pretransition zone

The experiment in Figure 5 shows that U_S has not remained unfolded in 1 s but has completely transformed into a partly folded, native-like intermediate, I_N. As expected for an intermediate less stable than the fully folded form of the protein, this intermediate unfolds considerably faster than the fully folded form, N. Figure 5 shows that I_N disappears at a rate marginally faster than the rate of formation of N from U_S. A similar result was reported for BSCCAA (Schreiber & Fersht, 1993b) and led to

the proposal of Mechanism 2 for the folding of U_S. To formally demonstrate the validity of Mechanism 2, it is necessary to demonstrate not only that the rate of formation of I_N is faster than that of N but also that the rate of formation of N is maximal when the population of I_N is at a maximum. The data in Figure 2A suggest that the $U_S \rightarrow I_N$ reaction occurs with a rate constant of 15 s^{-1} in 1.2 M GdnHCl, and therefore the temporal resolution of the data shown in Figure 5, or of that reported in the earlier study on BSCCAA (Schreiber & Fersht, 1993b), is insufficient to observe the formation of I_N. The rate of disappearance of I_N is similar to the rate of appearance of N (Fig. 5), strongly indicating that I_N is an intermediate on the folding pathway of U_S and that the observed rate is therefore the rate of the $I_N \rightarrow N$ transition. The overall $U_S \rightarrow N$ reaction is slow because the rate-limiting step, the $I_N \rightarrow N$ reaction, is slow.

The 3-state model does not correctly predict α_1 in the pre-transition zone. α_1 does not remain constant but decreases sharply with a decrease in GdnHCl concentration below 1.9 M. The value of λ_1 also is not constant at k_{12} but increases approximately 2-fold with a decrease in GdnHCl concentration in the pretransition zone. Similar GdnHCl-dependencies have been previously seen for α_1 and λ_1 in the case of BSCCAA (Schreiber & Fersht, 1993b). In both of the cases, inclusion of the native-like intermediate, I_N, on the folding pathway (Mechanism 2) can account for both the decrease in α_1 and increase in λ_1. In the case of barstar, with the assumption that the refolding rate constant starting from U_S is the rate constant for the formation of I_N (see above), the rate constants for the formation and unfolding of I_N in 1.2 M GdnHCl are 15 s^{-1} (Fig. 2A) and 1 s^{-1} (Fig. 4B), respectively, whereas in 0.6 M GdnHCl, they are 25 s^{-1} and 0.8 s^{-1}, respectively. I_N is therefore approximately 2.5-fold more stable in 0.6 M GdnHCl than in 1.2 M GdnHCl. Thus, the $U_S \rightleftharpoons I_N$ equilibrium shifts to favor I_N as the GdnHCl concentration is decreased. Because the reaction occurs with a GdnHCl concentration-independent rate constant of 16×10^{-3} s^{-1} (Fig. 5), and the $U_S \rightarrow U_F$ reaction occurs with a slower rate constant ($k_{12} = 5.3 \times 10^{-3}$ s^{-1}), the 2-fold increase in λ_1 with a decrease in GdnHCl concentration is expected. If the rate of the $I_N \rightarrow N$ reaction were the same as k_{12}, then λ_1 would have been expected to remain constant in the pretransition region, which is seen in the case of other proteins (Goto & Hamaguchi, 1982). The increase in λ_1 with decreasing GdnHCl concentration in the pretransition region has also been observed for ribonuclease A (Nall et al., 1978). The decrease in α_1 can also be explained by the shift in the equilibrium between U_S and I_N to favor I_N. This decrease in α_1 with a decrease in concentration of GdnHCl shows a midpoint at 1.2 M GdnHCl and, as in the case of the constant fragment of an immunoglobulin light chain (Goto & Hamaguchi, 1982), approximately represents the melting curve of I_N. Because I_N possesses native-like structure (Schreiber & Fersht, 1993b), the sharp decrease in α_1, which is observed (Fig. 2C), is expected. It should be noted that there is no change in fluorescence accompanying the $I_N \rightarrow N$ reaction (see above and Schreiber & Fersht [1993b]), and the slow phase observed in the direct folding experiments of Figure 2B in the pretransition zone does not represent the kinetics of this reaction.

The rate constant for *trans–cis* proline isomerization in the native-like intermediate, I_N (the $I_N \rightarrow N$ reaction), which is measured to be 16×10^{-3} s^{-1}, is more than 3 times faster than the rate constant of *trans–cis* proline isomerization in the unfolded

state (the $U_S \rightarrow U_F$ reaction), which was measured to be 5.3×10^{-3} s^{-1}. Proline isomerization is speeded up 40-fold in the native-like folding intermediate I_N on the folding pathway of ribonuclease A (Cook et al., 1979; Schmid, 1986b) but is unaffected by structure in the case of ribonuclease T1 (Kiefhaber & Schmid, 1992). Surprisingly, in the case of BSCCAA, it appears that structure does not speed up the proline isomerization reaction (Schreiber & Fersht, 1993b). It is possible that the free cysteine sulfhydryl groups in barstar may catalyze proline isomerization through hydrogen bonds with the imide nitrogen and/or the carbonyl oxygen of the proline. Such intramolecular catalysis of proline isomerization has been observed in the case of dihydrofolate reductase (Texter et al., 1993), where an arginine side chain was similarly implicated.

The rate constants and amplitudes of folding and unfolding of barstar at pH 7, with GdnHCl as the denaturant, which are reported here, are similar to those reported earlier for BSCCAA (Schreiber & Fersht, 1993b) at pH 8, with urea as the denaturant. In the latter case, a quantitative analysis of the folding and unfolding kinetics in the transition zone was, however, not carried out. In this paper, it has been shown that a quantitative analysis is possible for the GdnHCl-induced denaturation of barstar and that the validity of such an analysis can be tested by predicting the values of k_{12} and k_{21} and demonstrating that these values are independent of GdnHCl concentration. At present, the role of Pro 48 in the folding of barstar is being studied in our laboratory using Pro 48 → Ala 48 mutant protein. The quantitative analysis of the folding pathway in the transition and posttransition zones reported here will also allow a detailed analysis of the role of the very early intermediate, I_1, on the folding pathway at low concentrations of GdnHCl. Such work is also currently in progress.

Materials and methods

Protein purification

The barstar expression plasmid pMT316 was the generous gift of R.W. Hartley (1988). The method used to purify barstar has been described previously (Khurana & Udgaonkar, 1994). Protein concentrations were measured using an extinction coefficient of 23,000 M^{-1} cm^{-1} (Khurana & Udgaonkar, 1994).

Buffers

Both equilibrium and kinetic experiments were carried out in a buffer containing 5 mM sodium phosphate, 250 μM EDTA, and 1 mM DTT at pH 7 (native buffer), 25 °C. Different concentrations of GdnHCl were incorporated in the buffer as required. All experiments were done with barstar in reducing conditions, in the presence of 1 mM DTT. The presence of DTT prevents the small amount (<5%) of dimer formation through an intermolecular disulfide bond that is seen in nonreducing conditions (V. Raghunathan, V. Gupta, R. Khurana, J.B. Udgaonkar, & D. Salunke, unpubl. results). Any intramolecular disulfide bond formation or mixed disulfide bond formation is also prevented. To confirm this, for some unfolding experiments, barstar was first reduced with DTT on a G-25 column and the protein allowed to refold completely in the presence of 1 mM DTT. The protein reduced in this manner had identical unfolding kinet-

ics to barstar that had been directly reduced with 1 mM DTT (data not shown).

Equilibrium experiments

GdnHCl-induced equilibrium-unfolding curves of barstar at 25 °C were obtained in a concentration range of 0–6 M GdnHCl. Fluorescence was monitored at 320 nm on excitation at 287 nm using a Jasco FP-777 spectrofluorimeter. Both excitation and emission band widths were set at 5 nm.

Kinetic experiments

Rapid mixing experiments were done on a Biologic SFM-3 stopped-flow machine. Fluorescence was excited at 287 nm with a band width of 20 nm and monitored at 320 nm using a band-pass filter with a band width of 10 nm. Two detection channels were used so that the kinetics could be monitored over 2 different time domains for the same mixing event. For folding experiments, barstar was unfolded in 6 M GdnHCl for at least 2 h prior to the measurement and folding was initiated by a 2–20-fold dilution of the protein solution. For unfolding experiments, barstar concentrations used were typically 3 μM. Whenever possible, the kinetics were also monitored by manual mixing experiments on the Jasco spectrofluorimeter.

Data analysis

Equilibrium denaturation data were fitted by nonlinear least-squares analysis to a 2-state (N $\rightleftharpoons$ U) unfolding transition described by Santoro and Bolen (1988). This model leads to the following equation:

$$f_N = \frac{Y_O - (Y_U + m_U[D])}{(Y_N + m_N[D]) - (Y_U + m_U[D])}$$

$$= \frac{1}{1 + e^{-(\Delta G(H_2O) - m_G[D])/RT}}, \quad (1)$$

where f_N is the apparent fraction of folded protein, Y_O is the value of the spectroscopic property being measured at a denaturant concentration $[D]$; and Y_N and Y_U represent the intercepts, and m_N and m_U the slopes of the native and unfolded baselines of the raw fluorescence data, respectively. $\Delta G(H_2O)$ corresponds to the free energy difference between the folded and unfolded states in the absence of any denaturant, and m_G is a measure of the cooperativity of the unfolding reaction. Equation 1 assumes a linear dependence of $\Delta G(D)$ on the denaturant concentration $[D]$ (Schellman, 1978):

$$\Delta G(D) = \Delta G(H_2O) - m_G[D]. \quad (2)$$

$\Delta G(H_2O)$ and m_G are therefore the intercept and the slope, respectively, of the plot of the free energy of unfolding versus denaturant concentration. The concentration of denaturant at which the protein is half unfolded (when $\Delta G(D) = 0$) is given by C_M, and from Equation 2, $\Delta G(H_2O) = C_M m_G$.

Folding kinetics in the pretransition and transition regions could be described by a 2-exponential process:

$$F(t) = F(\infty) - F_1 \exp(-\lambda_1 t) - F_2 \exp(-\lambda_2 t). \quad (3)$$

Unfolding kinetics in the transition region were also described by a 2-exponential process:

$$F(t) = F(\infty) + F_1 \exp(-\lambda_1 t) + F_2 \exp(-\lambda_2 t), \quad (4)$$

where λ_1 and λ_2 are the apparent rate constants of the slow and fast phases, and F_1 and F_2 are the respective amplitudes. The relative amplitude of the slow phase is given by $\alpha_1 = F_1/(F_1 + F_2)$, and the corresponding relative amplitude of the fast phase is then given by $\alpha_2 = 1 - \alpha_1$. In the case of manual mixing experiments, α_1 at any GdnHCl concentration was determined by dividing the amplitude of the observed slow phase by the equilibrium amplitude of the reaction at that GdnHCl concentration.

Unfolding kinetics in the posttransition region could be described by a single exponential process: Equation 4 was used with F_1 set to zero.

The dependence of λ_2 on GdnHCl concentration, in either the pretransition region or the posttransition region, is given by the following equation (Tanford, 1970):

$$\log \lambda_2 = \log \lambda_2(H_2O) + m_{\lambda_2}[D], \quad (5)$$

where $\lambda_2(H_2O)$ is the rate constant of the fast phase when the protein is either unfolded or refolded in water.

All data were fit using the Biologic Biokine software or the SigmaPlot version 4.02 software.

Three-state kinetic analysis

The 3-state model (Mechanism 3) incorporating 2 unfolded forms, U_F and U_S, and the fully folded protein, N, was used to analyze the folding and unfolding kinetics in the transition and posttransition zones:

$$U_s \underset{k_{21}}{\overset{k_{12}}{\rightleftharpoons}} U_F \underset{k_{32}}{\overset{k_{23}}{\rightleftharpoons}} N. \quad \text{(Mechanism 3)}$$

In this model, U_F is the fast-refolding and U_S the slow-refolding species. The model is characterized by the 4 microscopic rate constants k_{12}, k_{21}, k_{23}, k_{32}, and the 2 equilibrium constants: K_{21} ($=k_{21}/k_{12}$) and K_{32} ($=k_{32}/k_{23}$).

The equations relating the 2 observed rate constants, λ_1 and λ_2, and the relative amplitude of the slow phase, α_1, to the 4 microscopic rate constants and the 2 equilibrium constants are well known (Hagerman & Baldwin, 1976):

$$\lambda_1 + \lambda_2 = k_{12} + k_{21} + k_{23} + k_{32} \quad (6)$$

$$\lambda_1 \lambda_2 = k_{12} k_{23} + (k_{12} + k_{21}) k_{32} \quad (7)$$

$$\alpha_1 = \frac{\dfrac{\lambda_2 |\lambda_1 - (k_{12} + k_{21})|}{\lambda_1 |\lambda_2 - (k_{12} + k_{21})|}}{\left[1 + \dfrac{\lambda_2 |\lambda_1 - (k_{12} + k_{21})|}{\lambda_1 |\lambda_2 - (k_{12} + k_{21})|}\right]}. \quad (8)$$

According to the 3-state model, when K_{21} is independent of GdnHCl concentration, and when the $U_S \rightleftharpoons U_F$ reaction is silent spectroscopically, α_1 is independent of the initial conditions and is expected to be the same whether determined from a folding or an unfolding experiment to the same final conditions.

Under the limiting conditions of $\lambda_2 \gg \lambda_1$, and $k_{23}, k_{32} \gg k_{12}, k_{21}$, Equations 6, 7, and 8 simplify to Equations 9, 10, and 11, respectively (Hagerman & Baldwin, 1976):

$$\lambda_1 = k_{12} + \frac{k_{21}}{1 + K_{23}} \qquad (9)$$

$$\lambda_2 = k_{23} + k_{32} \qquad (10)$$

$$\alpha_1 = \frac{f_N K_{21}}{1 + f_N K_{21}}, \qquad (11)$$

where f_N, the fraction of protein present as native protein in the final conditions, is given by:

$$f_N = \frac{1}{1 + K_{32}(1 + K_{21})} = \frac{1}{1 + K_{app}} \qquad (12)$$

$$= \frac{k_{12} k_{23}}{\lambda_1 \lambda_2}. \qquad (13)$$

K_{app}, the apparent equilibrium constant for unfolding of native protein to total unfolded protein, is equal to $([U_S] + [U_F])/N$.

Acknowledgments

References

Brandts JF, Halvorson HR, Brennan M. 1975. Consideration of the possibility that the slow step in protein denaturation reactions is due to *cis-trans* isomerization of proline residues. *Biochemistry 14*:4953–4963.

Cook KH, Schmid FX, Baldwin RL. 1979. Role of proline isomerization in folding ribonuclease A at low temperatures. *Proc Natl Acad Sci USA 76*:6157–6161.

Evans PA, Radford SE. 1994. Probing the structure of folding intermediates. *Curr Opin Struct Biol 4*:100–106.

Garel JR, Baldwin RL. 1973. Both the fast- and slow-refolding reactions of ribonuclease A yield native enzyme. *Proc Natl Acad Sci USA 70*:3347–3350.

Garel JR, Nall BT, Baldwin RL. 1976. Guanidine-unfolded state of ribonuclease A contains both fast- and slow-refolding species. *Proc Natl Acad Sci USA 73*:1853–1857.

Goto Y, Hamaguchi K. 1982. Unfolding and refolding of the constant fragment of the immunoglobulin light chain. *J Mol Biol 156*:891–910.

Grathwohl C, Wüthrich K. 1976. The X-pro peptide bond as an NMR probe for conformational studies of flexible linear peptides. *Biopolymers 15*:2025–2041.

Guillet V, Lapthorn A, Fourniat J, Benoit JP, Hartley RW, Mauguen Y. 1993a. Crystallization and preliminary X-ray investigation of barstar, the intracellular inhibitor of barnase. *Proteins Struct Funct Genet 17*:325–328.

Guillet V, Lapthorn A, Hartley RW, Mauguen Y. 1993b. Recognition between a bacterial ribonuclease barnase, and its natural inhibitor, barstar. *Structure 1*:165–176.

Hagerman PJ. 1977. Kinetic analysis of reversible protein folding reaction of small proteins: Application to the folding of lysozyme and cytochrome *c*. *Biopolymers 16*:731–747.

Hagerman PJ, Baldwin RL. 1976. A quantitative treatment of the kinetics of the folding transition of ribonuclease A. *Biochemistry 15*:1462–1473.

Hartley RW. 1988. Barnase and barstar. Expression of its cloned inhibitor prevents expression of a cloned ribonuclease. *J Mol Biol 202*:913–915.

Hartley RW. 1993. Directed mutagenesis and barnase-barstar recognition. *Biochemistry 32*:5978–5984.

Herning T, Yutani K, Taniyama Y, Kikuchi M. 1991. Effects of proline isomerization on the unfolding and refolding of human lysozyme: The slow refolding kinetic phase does not result from proline *cis-trans* isomerization. *Biochemistry 30*:9882–9891.

Kelley RF, Richards FM. 1987. Replacement of proline-76 with alanine eliminates the slowest kinetic phase in thioredoxin folding. *Biochemistry 26*:6765–6774.

Khurana R, Udgaonkar JB. 1994. Equilibrium unfolding studies of barstar: Evidence for an alternative conformation which resembles a molten globule. *Biochemistry 33*:106–115.

Kiefhaber T, Grunert HP, Hahn U, Schmid FX. 1990. Replacement of *cis* proline simplifies the mechanism of ribonuclease T1 folding. *Biochemistry 29*:6475–6480.

Kiefhaber T, Kohler HH, Schmid FX. 1992. Kinetic coupling between protein folding and prolyl isomerization. I. Theoretical methods. *J Mol Biol 224*:217–229.

Kiefhaber T, Schmid FX. 1992. Kinetic coupling between protein folding and prolyl isomerization. II. Folding of ribonuclease A and ribonuclease T1. *J Mol Biol 224*:231–240.

Kim PS, Baldwin RL. 1990. Intermediates in the folding reaction of small proteins. *Annu Rev Biochem 59*:631–660.

Kuwajima K. 1992. Protein folding in vitro. *Curr Opin Biotechnol 3*:462–467.

Lubienski MJ, Bycroft M, Jones DNM, Fersht AR. 1993. Assignment of the backbone. ^{1}H and ^{15}N NMR resonances and secondary structure characterization of barstar. *FEBS Lett 332*:81–87.

Matouschek A, Fersht AR. 1991. Protein engineering in analysis of protein folding pathways and stability. *Methods Enzymol 202*:82–112.

Matthews CR. 1993. Pathways of protein folding. *Annu Rev Biochem 62*:653–683.

Nakano T, Antonino LC, Fox RO, Fink AL. 1993. Effect of proline mutations on the stability and kinetics of folding of staphylococcal nuclease. *Biochemistry 32*:2534–2541.

Nall BT, Garel JR, Baldwin RL. 1978. Test of the extended two-state model for the kinetic intermediates observed in the folding transition of ribonuclease A. *J Mol Biol 118*:317–330.

Roder H, Elöve GA, Englander SW. 1988. Structural characterization of the folding intermediate in cytochrome *c* by H-exchange labelling and proton NMR. *Nature 335*:700–704.

Santoro MM, Bolen DW. 1988. Unfolding free energy changes determined by the linear extrapolation method. 1. Unfolding of phenylmethylsulfonyl α-chymotrypsin using different denaturants. *Biochemistry 27*:8063–8068.

Schellman JA. 1978. Solvent denaturation. *Biopolymers 7*:1305–1322.

Schmid FX. 1983. Mechanism of folding of ribonuclease A. Slow folding is a sequential reaction via structural intermediates. *Biochemistry 22*:4690–4696.

Schmid FX. 1986a. Fast-folding and slow-folding forms of unfolded proteins. *Methods Enzymol 131*:70–82.

Schmid FX. 1986b. Proline isomerization during refolding of ribonuclease A is accelerated by the presence of folding intermediates. *FEBS Lett 198*:217–220.

Schmid FX, Baldwin RL. 1979. The rate of interconversion between the two unfolded forms of ribonuclease A does not depend on guanidinium chloride concentration. *J Mol Biol 133*:285–287.

Schreiber G, Fersht AR. 1993a. Interaction of barnase with its polypeptide inhibitor barstar studied by protein engineering. *Biochemistry 32*:5145–5150.

Schreiber G, Fersht AR. 1993b. The refolding of *cis*- and *trans*-peptidyl prolyl isomers of barstar. *Biochemistry 32*:11195–11203.

Schultz DA, Schmid FX, Baldwin RL. 1992. *cis*-Proline mutants of ribonuclease A. II. Elimination of the slow refolding species by mutation. *Protein Sci 1*:917–924.

Tanford C. 1970. Protein denaturation. Part C. Theoretical models for the mechanism of denaturation. *Adv Protein Chem 21*:1–95.

Texter FL, Spencer DB, Rosenstein R, Matthews CR. 1993. Intramolecular catalysis of a proline isomerization reaction in the folding of dihydrofolate reductase. *Biochemistry 31*:5687–5691.

Udgaonkar JB, Baldwin RL. 1988. NMR evidence for an early intermediate in the folding pathway of ribonuclease A. *Nature 335*:694–699.

Utiyama H, Baldwin RL. 1986. Kinetic mechanism of protein folding. *Methods Enzymol 131*:51–70.